International Journal of Aeronautical and Space Sciences
https://doi.org/10.1007/s42405-024-00723-7

IJASS International Journal of Aeronautical and Space Sciences

ORIGINAL PAPER

Thermal Penetration of Aircraft Tyre Tread at Touchdown

Yu Li[1] · **Weiji Wang**[1]

Received: 23 March 2023 / Revised: 30 January 2024 / Accepted: 25 February 2024

Abstract
Most studies of friction and heat conduction in aircraft tyres at touchdown are limited to the tread surface. However, it is necessary to know the thermal penetration inside the tread to study the quantity of the potential decomposed and lost material by the frictional heat. Additionally, a high tread surface temperature does not necessarily guarantee a stronger thermal penetration inside the tread because of several factors. Therefore, it is necessary to establish a relationship between the tyre tread surface temperature and the internal heat penetration under the aircraft touchdown scenario. A model is established on MATLAB to simulate the aircraft tyre dynamics and tread heat conduction at touchdown. This model is capable of calculating the temperature increase in the tread, both on the surface and inside. It can also be used to determine the depth of thermal decomposition caused by frictional heat. Additionally, the study found that the Thermal Decomposition Depth to Surface Temperature Ratios (DTRs) are similar across the tread (the depth of thermal decomposition at each part of the tread surface is proportional to the surface temperature). Therefore, it can estimate the thermal penetration throughout the tread by simply calculating the surface temperature of the entire tread and the average DTR at several points of interest. The study provides a more straightforward approach for aircraft tyre thermal wear prediction and future research.

Keywords Aircraft tyre · Aircraft touchdown · Tyre heat conduction · Thermal penetration

Abbreviations

TDD	Thermal decomposition depth
DTR	Thermal decomposition depth to surface temperature ratio

1 Introduction

The aircraft tyres experience rapid and strong friction at touchdown. The frictional energy converts to heat and penetrates inside the tread. When the tread material temperature exceeds its critical point, thermal decomposition can result in a lower tread strength and loss of material, which is generally considered as tyre thermal wear [1, 2].

Saibel et al. suggested that 200 °C could be considered the critical point when studying aircraft tyre thermal wear. This level of temperature can provide enough energy to break all the bond linkages in the rubber structure [1]. The Goodyear test observed changes in the properties of tyre treads. Rubber will revert beyond 140 °C. At this stage, both tyre strength and adhesion drop significantly. After reaching 200 °C, rubber reverts to an uncured state and starts to degrade [3]. British Airways recorded an average material loss of 78 g on an Airbus A320 tyre per landing. However, Dunlop observed a value of 230 g, and Michelin reported 154 g [4]. Research from airlines, airports, and tyre manufacturers reveals that aircraft tyres degrade upon landing. The resulting lost rubber particles in the atmosphere damage the environment, and a thin tread also affects flight safety. One important physical quantity is the depth of decomposition. The depth of thermal wear at any point on the tread can also be referred to as the Thermal Decomposition Depth (TDD).

Several studies have attempted to solve the tyres' thermal problem in the past. Konde used FEA software to study the friction and tread temperature changes of aircraft tyres at a fixed sliding speed [5]. Alroqi used ANSYS to replicate Konde's experiment under the same conditions, achieving good agreement. Alroqi then believed that FEA and semi-infinite body model could be used as a method to study tyre temperature changes and launched subsequent research [6].

✉ Yu Li
yl697@sussex.ac.uk

[1] University of Sussex, Brighton, UK

Published online: 29 March 2024

Zakrajsek's team from USAF used FEA models and experimental equipment to study F-16 fighter tyre temperature rise and wear under non ideal landing conditions, such as a cross wind [7]. Our previous research [2] has also shown that the developed FEA model is capable of simulating tyre friction and surface temperature changes, and the results were confirmed experimentally.

As demonstrated above, FEA and semi-infinite body models are capable of solving tyres' thermal problem. Nevertheless, these studies have traditionally concentrated solely on the tread surface temperature. Due to the low thermal conductivity of the tread material, which hinders the effective penetration of frictional heat to a sufficient depth, FEA requires higher precision meshing and more computational time to calculate internal heat conduction. Consequently, solving temperature changes inside tyres can be challenging and few studies have focused on this. However, without solving the tyres' internal temperature change, we are unable to obtain information about TDD, let alone predict the thermal wear of the tyre. Therefore, we developed a completely new and quick methodology to predict temperature changes inside tyres without compromising the results accuracy.

It is worth mentioning that the tyre surface temperature itself does not solely reflect TDD. A more detailed demonstration will be provided in the results section.

The objectives of this study will be:

(1) Calculate surface and internal temperature changes for a simplified semi-infinite body friction model using Laplace's equation and demonstrate the influence of friction quantities, including heat duration and friction speed, on thermal penetration.
(2) Calculate surface and internal temperature changes based on aircraft tyre touchdown scenario and observe the surface temperatures, heat penetrations and the Thermal Decomposition Depth and Surface Temperature Ratio (DTR).
(3) Discuss the tread surface temperature, TDD and DTR under various landing scenarios, and identify any relationships between them and the friction quantities.

2 Modelling

2.1 Tyre Dynamic Modelling

The aircraft landing gear can be treated as a mass-spring-damper system with *2-DoF* (Degree of Freedom) as Fig. 1 shows.

m_1, m_2 are the tyre mass and load, $2k_1, k_2$ are the stiffness of the tyre and shock absorber (Note that each set of undercarriage has two tyres); c is the damping ratio of absorber;

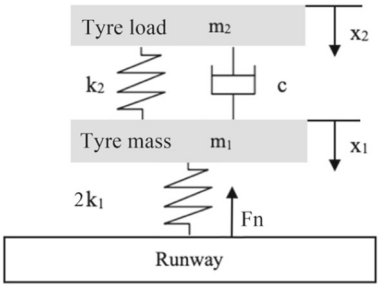

Fig. 1 The layout of landing gear 2-DoF system

and x_1, x_2 are the displacements of tyre and absorber. The ODEs (ordinary differential equations) of each mass will be:

$$m_2\ddot{x_2} + C(\dot{x_2} - \dot{x_1}) + k_2(x_2 - x_1) - m_2 \cdot g = 0 \tag{1}$$

$$m_1\ddot{x}_1 + C(\dot{x}_1 - \dot{x}_2) + x_1(2k_1 + k_2) - x_2k_2 - m_1 \cdot g = 0 \tag{2}$$

These ODEs can be solved when an initial condition is given: $x_1 = 0$, $\dot{x}_1 = \text{vs}$, $x_2 = 0$, $\dot{x}_2 = \text{vs}$, where vs is the aircraft vertical speed at touchdown. Then, the normal force of the tyre F_n will be:

$$F_n = k_1x_1/2 \tag{3}$$

The semi-length of contact surface L can also be found:

$$L = \sqrt{R^2 - (R - x_1)^2} \tag{4}$$

Equation 5 states a simplified method to calculate the tyre's effective radius R_e based on small angle approximation.

$$R_e = R - \frac{x_1}{3} \tag{5}$$

The contact surface of aircraft tyre should be an ellipse, with a fixed ratio of its major axis to its minor axis ε. Therefore, the tyre contact surface area A will be:

$$A = \pi \cdot \frac{AO^2}{\varepsilon} \tag{6}$$

The displace angle of the contact surface Φ is expressed as follows, and all the relative parameters are marked in Fig. 2.

$$\Phi = \sin^{-1}(L/R) \tag{7}$$

The Burckhardt Formula can be used to calculate the CoF (coefficient of friction) depending on the tyre slip ratio SR,

$$\mu = C_1\left(1 - e^{-C_2\text{SR}}\right) - C_3\text{SR} \tag{8}$$

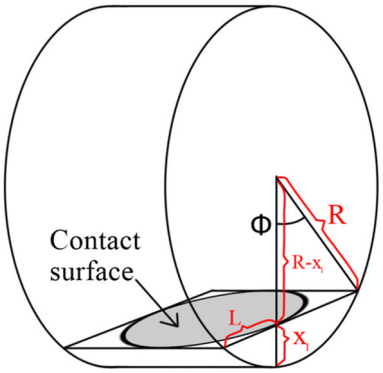

Fig. 2 The tyre deformation layout

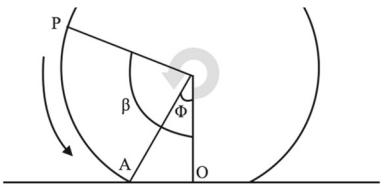

Fig. 3 The position of a point of interest P when entering the contact surface

where C_1 equals 1.28, C_2 equals 23.99 and C_3 equals 0.52 for aircraft tyre on a dry asphalt runway [8], SR $= 1-\omega R/v$, ω is the tyre's angular speed and v is the aircraft's speed.

The tyre friction F_x will be the product of CoF and tyre's normal force F_n, and the wheel angular acceleration α comes from the friction torque. The wheel angular speed ω is the integration of angular acceleration, while the wheel linear speed v_l is the product of angular speed and the tyre's effective radius.

$$F_x = F_n \cdot \mu \tag{9}$$

$$\alpha = \frac{F_x}{m_1 \cdot R_e} \tag{10}$$

$$\omega = \int_0^t \alpha dt \tag{11}$$

$$v_l = \omega \cdot R_e \tag{12}$$

2.2 Heat Conduction Modelling

The basic step of the heat generation modelling is to find out the friction timing of each point of interest around the entire tyre circumference to determine the experienced friction quantities.

Figure 3 shows a point of interest P on the circumference, β is its displaced angle to the contact surface centre O. The

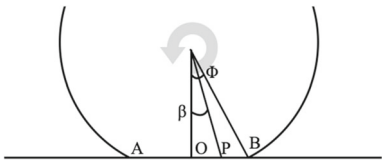

Fig. 4 The positions of P when leaving the contact surface

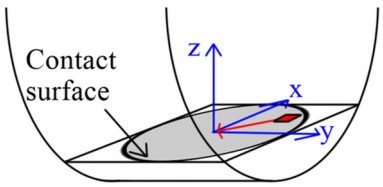

Fig. 5 The contact surface modelling for FEA, tyre spins anti-clockwise

value of β in Eq. 13 will reduces as the wheel spins anti-clockwise. When the value of β becomes less than Φ, P enters the contact surface, and the value of t will be its friction start time t_s.

$$\beta = \beta_0 - \int_0^t \omega dt \tag{13}$$

where β_0 is the initial value of β.

Later, P will move to the right side of the contact surface, illustrated in Fig. 4. When the value of β, expressed in Eq. 14, becomes larger than Φ, the friction ends, and the value of t will be the friction end time t_e. The friction duration of each point of interest will be $t_s - t_e$.

$$\beta = \int_0^t \omega dt - \beta_0 \tag{14}$$

For each point of interest, the experienced friction quantities will be the average values in the specific time interval, defined by t_s and t_e:

$$\overline{v_f} = \frac{1}{(t_e - t_s)/dt} \sum_{i=n}^{m} v_{fi} \tag{15}$$

$$\overline{F_x} = \frac{1}{(t_e - t_s)/dt} \sum_{i=n}^{m} F_{xi} \tag{16}$$

$$\overline{A} = \frac{1}{(t_e - t_s)/dt} \sum_{i=n}^{m} A_i \tag{17}$$

where $dt = 0.0001$, the time interval set in MATLAB, $m = t_e/dt$, $n = t_s/dt$.

The main idea of the FEA is to evenly divide the contact surface into many rectangular heat elements of equal size and calculate the heat contribution of each element. Figure 5 shows an example element in red colour. This element will

generate frictional heat and transfer it to the point of interest where the temperature change is measured.

If a surface point of interest locates at the origin of coordinate system and the example element locates at (x_u, y_u, 0), then the square of the distance between them will be: $r^2 = x_u^2 + y_u^2$. On the other hand, if we are going to measure the temperature of a point of interest inside the tread with a depth d and a coordinate of (x_u, y_u, d), then $r^2 = x_u^2 + y_u^2 + d^2$. r^2 will be substituted into the Laplace's equation to calculate the temperature rise θ. A general solution of Laplace's equation if we consider a continuous heat on the two-dimensional contact surface will be [9]:

$$\theta = \frac{q}{\rho c (4\pi a)^{\frac{3}{2}}} \int_0^t \int_{-L/2}^{L/2} \int_{-W/2}^{W/2} \frac{e^{-r^2/4a(t-\tau)}}{(t-\tau)^{\frac{3}{2}}} dx dy d\tau \tag{18}$$

where $\alpha = k/(\rho c)$, q is the heat liberation rate, ρ, c, k and α are the tread material's density, specific heat capacity, thermal diffusivity, and thermal conductivity, respectively. t is the total friction duration of the point of interest, τ is the time after the initiation of heat, incrementing at specific time intervals, dt.

This solution contains an integral part calculating the heat contribution of each element and integrates them over contact surface position and friction duration. The integration can only be solved numerically.

The heat liberation rate per heat element q is expressed in Eq. 17. 90% of frictional heat will go to the tyre tread, and the rest to the runway [10]. The number of heat elements N depends on the total contact surface area $\overline{A}$ and a unit element area, 10^{-9} m^2 or 1 mm^2. The unit element area is the result of a large number of tests, which ensures a balance between computational efficiency and result accuracy.

$$q = 0.9 F_x \cdot \overline{v_f} / N \tag{19}$$

After obtaining the temperature rise of every point of interest, we are able to determine the *TDD*, considering a 22 °C environment temperature. There will be no thermal decomposition or *TDD* if the surface temperature is below the critical point. Table 1 lists the required physical variables for the modelling.

Table 1 The required variables in the modelling

Parameter	Value	Note and sources
m_1	60 kg	Reasonable values of ERJ-175
m_2	17,000 kg	
R	0.48 m	H38 × 13.0–18 tyre
ε	1.6	Boeing research [11]
k_1	1.75×10^6 N/m	Comprehensive value of Alroqi [6] and NASA [12]
k_2	4×10^5 N/m	
C	6.25×10^5 N s/m	
ρ	1200 kg/m^3	Comprehensive value of Alroqi [6] and Konde [5]
k	0.15 W/m K	
c	2005 g K	

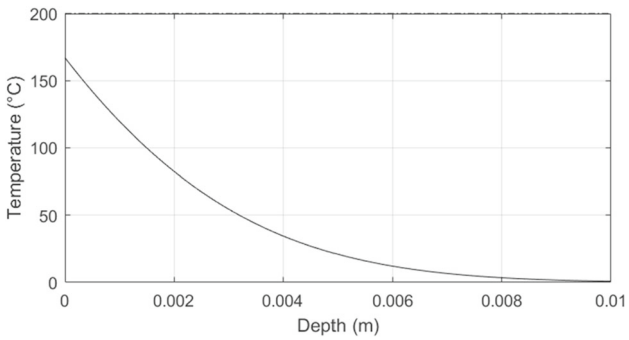

Fig. 6 Thermal penetration in a semi-infinite body

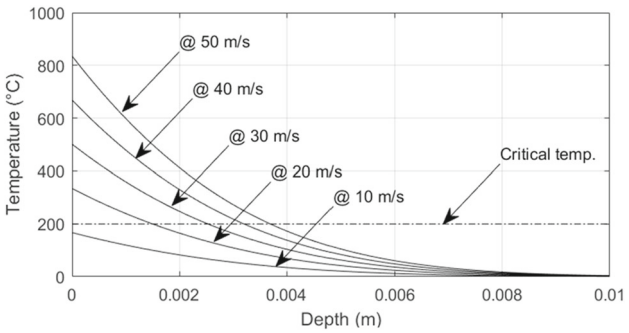

Fig. 7 Thermal penetration at different friction speeds

3 Results and Discussion

3.1 Analysis of Semi-infinite Body Model

Initially, a basic analysis is performed to observe the impact of each physical quantity on the tyre surface temperature and thermal penetration. For a constant friction speed of 10 m/s, a friction force of 200, 000N, a contact surface area of 0.01m^2, and a friction duration of 0.01s, the calculated surface temperature rise is 167 °C according to the Laplace's equation, and the thermal penetration plot is shown in Fig. 6. The temperature distribution inside the tread is non-linear, and the heat is transmitted to an effective depth of about 0.01 m in the given friction environment.

Figure 7 shows an example of thermal penetrations at different friction speeds. As the plot shows, the five curves from top to bottom represent the friction speed ranging from 50

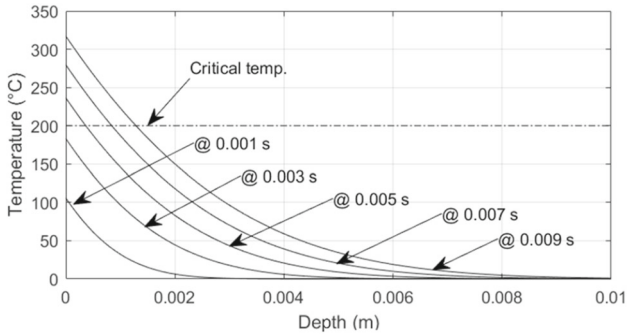

Fig. 8 Thermal penetration at different friction durations

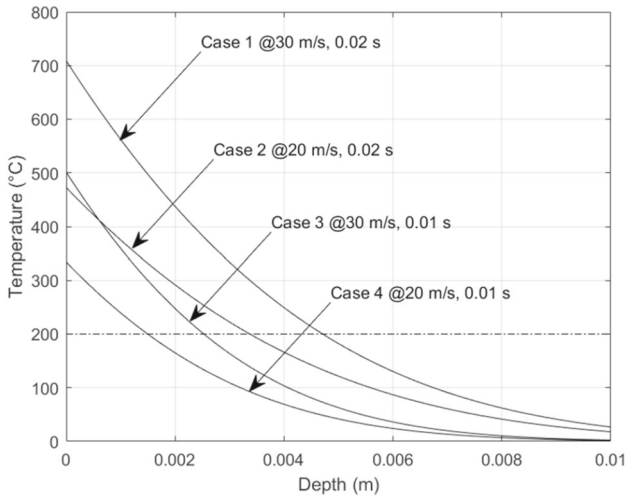

Fig. 9 Thermal penetration at different friction speeds and durations

to 10 m/s. A dotted line indicates the critical point. It can be observed that as friction speed increases, the surface temperature also increases, leading to higher temperatures at the same depth.

Furthermore, the duration of friction is changed from 0.001 to 0.009s, with the results illustrated in Fig. 8. The prolonged friction will not only elevate the surface temperature but also result in the continued penetration of heat into the body. Therefore, the curve appears to move upward and to the right as the duration extends. Specifically speaking, a friction duration of 0.0001 s results in a surface temperature of approximately 100°C and an effective penetration depth of about 0.003 m. However, these values increase to 320°C and 0.01 m for a friction duration of 0.009s.

These results show variation regularities when either friction speeds or durations change independently. However, the situation may be different when both factors are considered. Figure 9 shows the thermal penetration of four cases, which involve different combinations of friction speeds and durations.

When the friction speed and duration are at their lowest (Case 4) or highest (Case 1) levels, the thermal penetration curve is also at its lowest or highest position and does not interact with others. In Case 3, the surface temperature reaches 501°C, which is higher than the 473°C in Case 2. However, in Case 3, the TDD is 0.0025 m, which is less than the 0.0034m in Case 2.

It is evident that increasing both the friction speed and duration simultaneously can raise the tyre surface temperature and thermal penetration depth. However, predicting the change becomes challenging when one physical quantity increases while the other decreases. One possible explanation is that when we use Laplace's equation (Eq. 18) to calculate the temperature rise, the friction speed affects the magnitude of the constant part by altering q (Eq. 19), and the duration t as the upper limit of the integral affects the magnitude of the integral part. Consequently, when the effects of the two physical quantities are combined, it is difficult to determine which physical quantity has a greater impact, and there could be a mismatch in surface temperature and thermal penetration depth.

During aircraft touchdown, the friction force, contact area, and friction speed of the tread change continuously, accompanied by the vertical oscillation of the 2-DoF system. Each point of interest on the tread around the entire tyre circumference experiences a unique frictional environment with varying friction speed and duration. For example, at moment when the aircraft has just touched down, the friction speed of the tyres gradually decreases, and the friction time of the point of interest also reduces as the tyres spin up. However, when the lift of the aircraft disappears, the tyres are pressed further on the runway, expanding the contact surface area. In this case, the friction time of the point of interest may increase instead. This may result in a mismatch between the surface temperature of certain points of interest and the TDD. The calculated DTR has a high probability of being irregular and nonlinear, potentially resulting in no discernible relationship between the tyre surface temperature and internal temperature changes. As a consequence, the conditions for developing new methodology may be lost. Further tests are needed to address this problem.

3.2 Analysis of Aircraft Tyre Landing Friction Model

Figure 10 shows the calculated temperature of an aircraft tyre at touchdown with an ambient temperature of 22°C, the aircraft landing speed is 60 m/s or 117 kt, and the vertical speed is 0.5m/s or 98fpm. The maximum temperature is 391°C, located at 0 radians, which is the first point of contact with the runway at touchdown.

Figure 10 also shows the temperature at various depths below the tread surface, ranging from 0 to 0.02 m at consistent intervals of 0.001 m, resulting in a total of 21 sampling

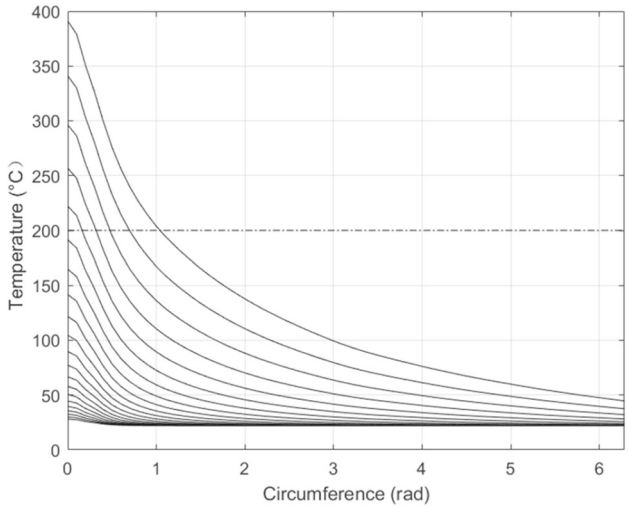

Fig. 10 Surface and interior temperatures around the entire tyre circumference

Table 2 The TDDs

Location	Surface temp	TDD
0 rad	391 °C	4.9 mm
0.2 rad	358 °C	4.1 mm
0.4 rad	294 °C	2.4 mm
0.6 rad	253 °C	1.5 mm
0.8 rad	224 °C	0.8 mm
1.0 rad	202 °C	0.2 mm
1.1 rad	194 °C	0 mm

depths. The higher the curve on the plot, the closer the point of interest is to the surface. No legend is provided because of the high density of the curve distribution. We can see from Fig. 10 that only certain parts of the tyre tread undergo thermal wear, and the temperature of most parts is lower than the critical point (as indicated by the dotted line in Fig. 10).

In addition, we measured the TDD of each point of interest on the tread, and the results are shown in Table 2. Data between 1.2 and $2\pi rad$ are not recorded because the temperature is not high enough to cause thermal wear. Table 2 illustrates that as the surface temperature increases, there is a greater amount of material undergoing thermal decomposition beneath the surface. TDD is given in millimetres.

Figure 11 displays the temperatures of various points of interest on the tread surface and their corresponding TDDs. It can be seen that the two quantities are directly proportional, with a Pearson linear correlation coefficient of 0.9998. The polynomial curve fitting function in MATLAB can be used to calculate the curve gradient automatically, yielding a value of 0.0247 for the case illustrated in Fig. 11. This means that if the temperature at the tread surface exceeds the critical point,

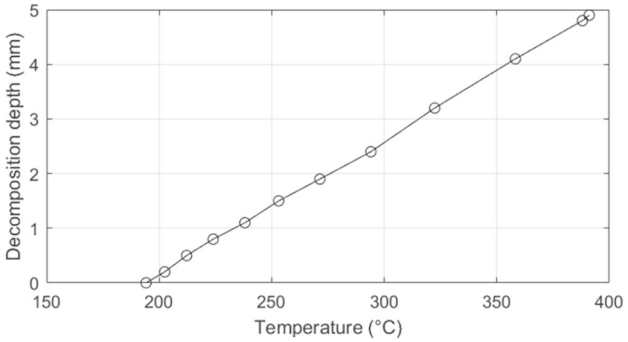

Fig. 11 Surface temperature and corresponding TDD ($r = 0.9998$)

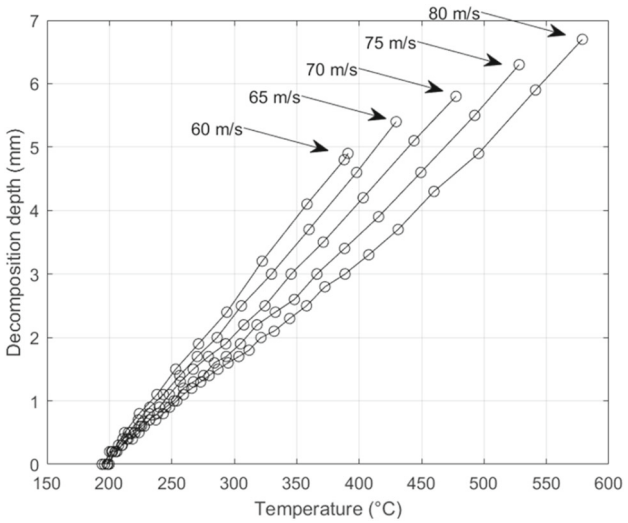

Fig. 12 Surface temperature and corresponding TDD at five landing speeds ($r = 0.9998, 0.9996, 0.9995, 0.9988, 0.9978$, sort by increasing landing speed)

then the *TDD* at this point is 0.0247 times the excess amount (unit: mm). The gradient is tentatively named Decomposition Depth to Surface Temperature Ratio (DTR).

Furthermore, we attempt to modify the landing speed and vertical speed to investigate their impact on TDD. Figures 12 and 13 illustrate the results. Both once again demonstrate the existence of a linear relationship between surface temperature and TDD with the assistance of Pearson linear correlation test, as well as the potential to obtain a DTR. It needs to be emphasized again that proportionality is extremely important for the calculation and application of DTR. By multiplying the tyre surface temperature with a single fixed DTR value, we can directly obtain TDD data, enabling a quicker prediction of thermal wear. If a linear relationship does not exist, it becomes challenging to establish a direct connection between surface temperature and TDD. This connection is the core idea of the new methodology we have developed.

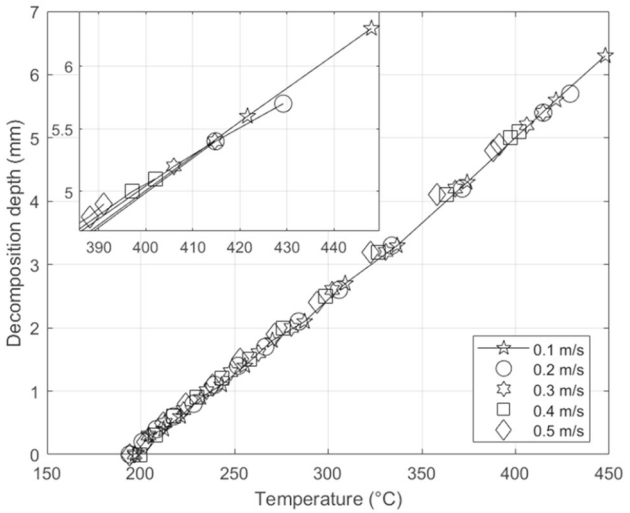

Fig. 13 Surface temperature and corresponding TDD at five vertical speeds ($r = 0.9992, 0.9996, 0.9995, 0.9997, 0.9998$, sort by increasing vertical speed)

Table 3 Relevant data for discussion

	vs = 0.5 m/s $v = 80$ m/s	vs = 0.5 m/s $v = 60$ m/s	vs = 0.1 m/s $v = 60$ m/s
t	0.0185s	0.0285s	0.0281 s
q	882×10^5 W	712×10^5 W	722×10^5 W
θ	200.8 °C	200.8 °C	202.0 °C

According to Fig. 12, it can be observed that the *DTR* decreases (the line becomes more horizontal) as landing speed increases. This suggests that the faster the aircraft lands, the smaller the TDD in the same temperature zone, resulting in less loss of tread material. One plausible explanation is that an increase in landing speed leads to an increase in the number of revolutions of the tyre. There is, therefore, more tread area to distribute the frictional heat. For example, at a landing speed of 60m/s, only the tread area between 0 and 1 rad has a positive *TDD*, but the range expands to 3.2 rad at 80 m/s.

Figure 13 displays the results at various vertical speeds. The smoother the aircraft lands, the higher the maximum temperature on the tread. However, DTR hardly changes in any scenario. The curves representing the five cases almost overlap. The subplot displays the maximum temperature and TDD for each case. Further studies are conducted to determine why vertical speed has little effect on DTR. Under three landing conditions, we look for points of interest with temperature rises closest to 200 °C and disclose their friction duration t and heat liberation rate per heat element q (Table 3).

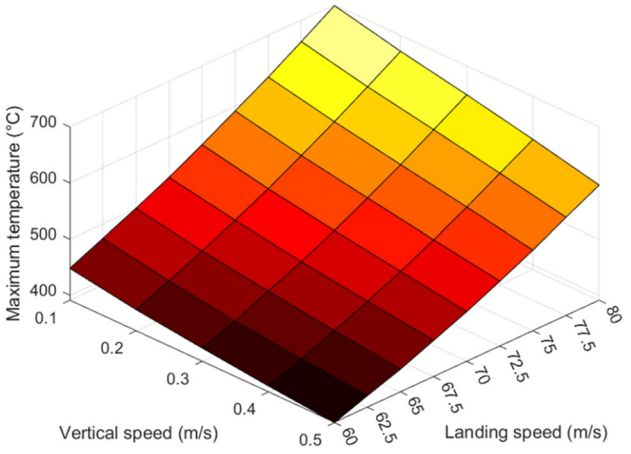

Fig. 14 Maximum tread temperature at different landing conditions

A change in landing speed will cause q to change at the same point of interest but will not affect t (determined only by tyre load). Therefore, for one point of interest on the faster landing tyre, we can find another point of interest on the slower tyre, smaller t but larger q, resulting in the same surface temperature changes. However, this does not imply that the internal temperature changes in the same way because both physical quantities change, as discussed in Chapter 3.1. Note that the *DTR* stability is not affected.

A change in vertical speed does not affect q. For the first few points of interest, t will change significantly because the vertical speed affects the 2-DoF system and the tyre load. However, such changes quickly disappear in the rear points of interest as tyre spins up. We speculate that although greater vertical speed results in greater tyre angular acceleration, the tyre contact area also increases due to the higher load. Therefore, the time for the point of interest to move across the contact surface does not change significantly. Therefore, vertical speed has little effect on q and t at the same point of interest. And according to Laplace's equation, we can conclude that internal temperature changes are also not affected, and DTR is constant. Regardless of how different factors affect DTR, as long as it is confirmed as a globally constant value, it can be used to predict TDD and thermal wear. More testing could be done to demonstrate the generality of the effect of vertical speed on DTR.

3.3 Analysis of Relationship Between Surface Temperature and Thermal Penetration

We are examining the impact of landing speed and vertical speed on tread temperature, TDD, and DTR. Figure 14 illustrates the maximum tread temperature at various landing and vertical speeds. For all tested conditions, the maximum tyre temperature exceeded the critical point of 200 °C, indicating the occurrence of thermal wear.

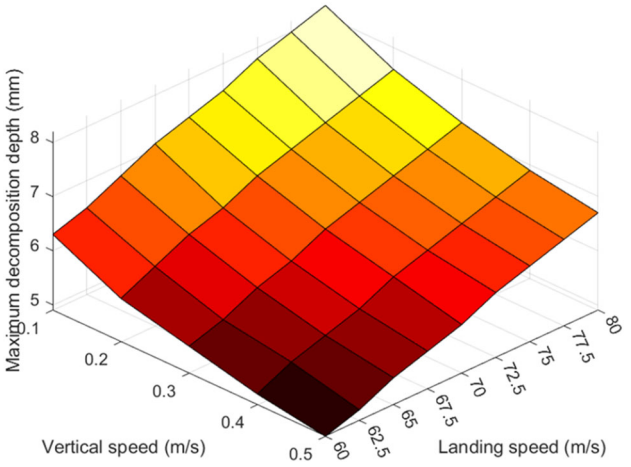

Fig. 15 Maximum TDD at different landing conditions

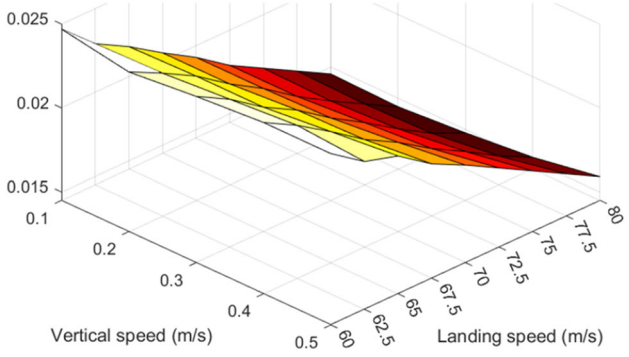

Fig. 16 DTR at different landing conditions

The results clearly show that faster and softer landings lead to higher temperatures. Higher landing (friction) speed increases q, which in turn raises tyre temperature. Lower vertical speed does reduce tyre friction level but also increases the tyre spin-up time, leading to higher temperatures. This is also confirmed in Alroqi's research [6].The temperature can reach 698 °C at a landing speed of 80m/s and a vertical speed of 0.1 m/s. On the other hand, the temperature will only reach 391°C at a landing speed of 60 m/s and a vertical speed of 0.5m/s. A linear correlation test is then conducted. The results indicate a strong linear relationship between the maximum temperature and both types of speed, with a Pearson correlation coefficient consistently exceeding 0.99.

The maximum TDD for each landing and vertical speed is shown in Fig. 15. Combined with Fig. 14, it can be observed that the higher the temperature of the tread surface, the greater the depth of thermal decomposition. The maximum TDD is reached at the highest landing speed and the lowest vertical speed, and vice versa. Therefore, the pilot needs to control the aircraft to achieve the heaviest and slowest landing in order to minimize tyre thermal wear, while staying within safety limits.

The linear correlation test continues to demonstrate a strong relationship between maximum TDD and landing speed, with a consistently high Pearson coefficient exceeding 0.99. Every 1 m/s increase in landing speed results in a 0.085 mm increase in maximum TDD in our landing environments. Additionally, maximum TDD and vertical speed demonstrate a non-linear relationship. It can be predicted that the maximum TDD will decrease and approach a constant value as the vertical speed tends towards infinity, based on the sequence of the data. However, this is not the case as a high vertical speed could cause the aircraft to bounce, leading to the tyres leaving the runway, creating an entirely different friction environment.

The results of the DTR are shown in Fig. 16. It should be noted that in any landing situation, the temperature of each point of interest on the tyre surface is proportional to its TDD, which is an essential condition for calculating an effective DTR. The results indicate a strong linear relationship between DTR and landing speed, as evidenced by a Pearson correlation coefficient of approximately 0.995. It also demonstrates that vertical speed has little effect on DTR, as depicted in Fig. 13.

It should be noted that the results are based on the assumption that the aircraft lands perfectly, for example, with all four tyres touching down simultaneously without bouncing or leaving the ground. When the tyres touch down non-simultaneously due to crosswind and other reasons, each tyre encounters a different friction environment. As a result, each DTR must be analysed separately. One question arises: will the sudden reduction in load on the first tyre touching the ground affect the DTR when the other tyres touch the ground later and share the aircraft load? When the tyres bounce, we need to consider its motion in the air, which may involve aerodynamic and rotational inertia issues. The model needs expansion, and tests need to be conducted to address these considerations and assess their impact on *DTR*. It needs to be emphasized again that in any scenario, as long as *DTR* is found to be a globally constant value, it can be used to predict TDD and thermal wear.

4 Conclusion

This study developed a model for aircraft tyre landing friction to investigate the surface temperature of the tyre, heat penetration, and their relationship.

First, the model illustrates a specific case in which the surface temperature does not correspond to the heat penetration, a phenomenon attributed to the coupling effect of two significant physical quantities: friction duration and friction speed. However, such instances were barely detected in a

series of tests, suggesting that both friction duration and friction speed generally decrease simultaneously across all areas of the tread. Although friction duration could theoretically increase (e.g., due to tyre deformation leading to a larger contact area), the data indicate that any such effect would be minimal. Therefore, the conflict between the impacts of these two physical quantities is unlikely to occur in the context of aircraft landings and remains primarily theoretical.

Second, we investigated the impact of aircraft landing and vertical speeds on tyre heat conduction. The results illustrate predominantly linear relationships between these speeds and tyre surface temperature and TDD, except for vertical speed, which has little effect on DTR.

Generally speaking, for the same tyre in the same landing scenario, we can infer the global fixed DTR by measuring only a portion of the tyre area and use that information to estimate the global TDD and thermal wear. Such a three-dimensional problem is addressed on an almost two-dimensional level. Compared to using FEA and other methods to measure temperature at different depths, the proposed method significantly reduces calculation time and is more easily adaptable for commercial applications without compromising reliability.

For example, we can install simple code on the aircraft computer to predict the tyre wear amount of each landing. This prediction is based on calculated DTR and the tyre surface temperature detected by the sensor. By combining this information with ground check results, we can forecast the tyre wear status and enhance flight safety. Additionally, as described in Chapter 3.3, we can use machine learning to identify the DTR change trends for the same tyre in various landing scenarios. This enables us to estimate wear more accurately. Such insights allow airlines, maintenance, and pilots to understand the impact that landing controls can have on tyre performance, durability and, ultimately, flight safety.

The limitation of this model is that it is not suitable for tyre rebound scenarios, which are very common. Additionally, only tricycle landing gear configurations containing four main tyres were considered. In the future, more tests are needed to verify whether, under different landing scenarios (including cross wind, bouncing, braking application, etc.) and with various landing gear configurations (such as the multi-wheel bogie of a wide-body aircraft, where each tyre is affected by the tilt angle and has different contact times with the ground), the DTR can still maintain a globally constant value.

Declarations

Conflict of interest Not applicable.

References

1. Saibel EA, Tsai C (1973) Tire wear by ablation. Wear 24(2):161–176. https://doi.org/10.1016/0043-1648(73)90229-9
2. Li Y, Wang W (2023) Temperature elevation of aircraft tyre surface at touchdown with pre-rotations. CEAS Aeronaut J. https://doi.org/10.1007/s13272-023-00652-3
3. Goodyear (2020) Aircraft tire care & maintenance. Available at https://www.goodyearaviation.com/resources/pdf/aviation-tire-care-2020.pdf. Accessed 10 Nov 2023
4. Morris KM (2006) An estimation of the tyre material erosion from measurements of aircraft tyre wear. British Airways Environmental Affairs Tech, ENV/ KMM/1131/14.18
5. Kondé AK, Rosu I, Lebon F et al (2013) Thermomechanical analysis of an aircraft tire in cornering using coupled ale and lagrangian formulations. Cent Eur J Eng 3:191–205. https://doi.org/10.2478/s1353101200496
6. Alroqi AA (2018) Investigation of the heat and wear of aircraft landing gear tyres. Doctoral thesis (PhD), University of Sussex
7. Zakrajsek AJ et al (2016) Aircraft tire spin up wear analysis through experimental testing and computational modeling. AIAA 2016 0413. 57th AIAA/ASCE/AHS/ASC structures, structural dynamics, and materials conference
8. Dousti M, Baslamisli S, Onder E, Solmaz S (2014) Design of a multiple-model switching controller for ABS braking dynamics. Trans Inst Meas Control. https://doi.org/10.1177/0142331214546522
9. Kuo WL, Lin JF (2006) General temperature rise solution for a moving plane heat source problem in surface grinding. Int J Adv Manuf Technol 31(3–4):268–277. https://doi.org/10.1007/s00170-005-0200-0
10. Rosu et al (2016) Experimental and numerical simulation of the dynamic frictional contact between an aircraft tire rubber and a rough surface. Lubricants 4(3):29. https://doi.org/10.3390/lubricants4030029
11. Boeing (2017) Calculating tire contact area. Retrieved from https://www.boeing.com/assets/pdf/commercial/airports/faqs/calctirecontactarea.pdf. Accessed 5 Oct 2023
12. Davis PA, Lopez MC (1988) Static mechanical properties of 30 x 11.5 14.5, type VI11 aircraft tires of bias ply and radial belted design. NASA, Hampton, Virginia, NASA Technical Paper 2810